Title

Magnetic-Current-Loop-Induced Electric Dipole Antenna Based on Substrate Integrated Waveguide Cavity

Authors
Wu, Chung-Tse Michael
Choi, Jun H
Lee, Hanseung
et al.

Publication Date
2014

DOI
10.1109/lawp.2014.2311410

Peer reviewed

Magnetic-Current-Loop-Induced Electric Dipole Antenna Based on Substrate Integrated Waveguide Cavity

Chung-Tse Michael Wu, *Student Member, IEEE*, Jun H. Choi, *Student Member, IEEE*, Hanseung Lee, *Student Member, IEEE*, and Tatsuo Itoh, *Life Fellow, IEEE*

***Abstract*—In this letter, a novel dipole antenna based on substrate integrated waveguides (SIWs) is presented. The dipole antenna radiates through the equivalent magnetic current loops on the top and bottom annular ring slot that is excited by the fundamental mode of the SIW cavity. Therefore, the proposed dipole possesses a vertical polarization perpendicular to the metallic plane. Moreover, thanks to normal electric field, the proposed dipole is less affected by the ground plane size and surrounding metal. The proposed antenna topology provides a very easy way to realize vertical dipole antenna by just using planar circuits and is promising to be used as a fundamental element to realize antenna arrays.**

***Index Terms*—Annular ring, antenna array, dipole antenna, magnetic current, substrate integrated waveguide.**

I. Introduction

DIPOLE antennas are the fundamental elements of antenna families [1]. Conventional ways of their realization are to use wires located in the free space and impose time-varying currents on them. Accordingly, the radiating characteristics of dipole antennas can be calculated analytically through the free-space Green's function, and the radiation patterns are shown to be well-known donut shapes. In addition, the polarization of a dipole antenna corresponds to the orientation of the wire.

Modern portable wireless communication devices, however, highly demand the ease of integration of antennas. As a consequence, printed antennas of low profiles are widely used in wireless handsets since they can be easily integrated with RF front ends. For instance, planar inverted-F antennas (PIFAs) are one of the most commonly used printed antennas nowadays in wireless applications, including cell phones, laptops, tablets, and vehicles [2]. The radiation mechanism of PIFAs pertains to that of a quarter-wavelength monopole antenna. Therefore, the polarization of such planar antennas is horizontal, i.e., parallel to the plane where the printed antenna is located.

It has been reported in the literature that microstrip patch antennas can be used to realize monopole-like radiation patterns [3]–[6]. However, these antennas usually need coaxial feeds to excite the correct higher-order modes in order to generate the desired monopole radiation patterns. It is also difficult for these approaches to produce dipole-like patterns due to the use of coaxial feeds and ground plane. On the other hand, substrate integrated waveguides (SIWs) offer a great solution to realize waveguide-like structures in printed circuits with simple feeding networks and low cost. It is reported that SIW antenna with ring slots loaded can provide circular polarizations [7], [8].

Manuscript received December 10, 2013; revised February 04, 2014; accepted March 10, 2014. Date of publication March 12, 2014; date of current version March 26, 2014.

The authors are with the Electrical Engineering Department, University of California, Los Angeles, Los Angeles, CA 90095 USA (e-mail: michael.wu@ucla.edu).

Color versions of one or more of the figures in this letter are available online at http://ieeexplore.ieee.org.

Digital Object Identifier 10.1109/LAWP.2014.2311410

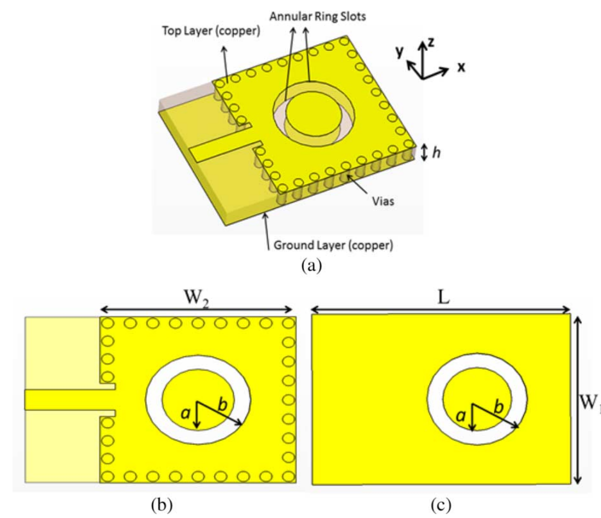

Fig. 1. Proposed antenna: (a) general topology, (b) top view, and (c) bottom view.

In this letter, a simple but useful approach to generate vertical dipole patterns using SIW structures is presented. The annular slot rings loaded on the top and bottom side of an SIW cavity are excited at the waveguide cavity's fundamental mode (TE_{101}). The resulting equivalent magnetic current will create a dipole-like pattern in the free space. The radiating mechanism will be explained analytically; the simulated and measured results of the proposed antenna show a great agreement. Such antennas are promising to be further used in low-profile planar antenna arrays with the needs of vertical polarization. Potential applications for the proposed antenna can be its use as external drop-in antennas for mobile devices or PCs.

II. Antenna Topology and Theory

A. Antenna Topology

Fig. 1 illustrates the topology of the proposed magnetic-current-loop-induced dipole antenna. The top and bottom layer contain identical annular ring slots in order to form equivalent magnetic currents. The vias are used to form walls to create

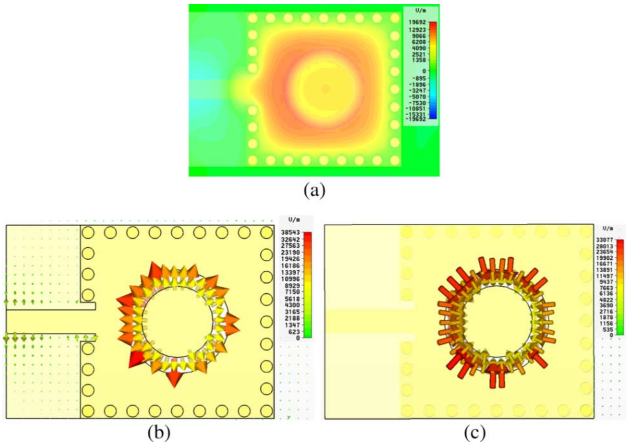

Fig. 2. Electric field distribution of (a) inside the cavity, (b) top layer, and (c) bottom layer.

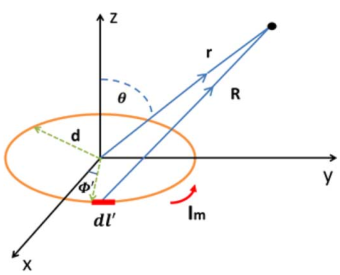

Fig. 3. Geometry of circular magnetic current loop.

the SIW cavity. The electric (E) field distribution of the SIW cavity is plotted in Fig. 2. The cavity is excited at its fundamental mode (TE_{101}-like mode), which can be observed from Fig. 2(a). It is noted that the E-fields on the annular ring slots on the top and bottom layers are oriented at opposite directions as shown in Fig. 2(b) and (c). However, since the normal vectors of the top and bottom surface are also opposite, the equivalent magnetic currents, i.e., $\vec{M} = \hat{n} \times \vec{E}$, will flow in the same directions both on the top and bottom layers.

B. Radiated Fields

To find the fields radiated by the proposed magnetic-current-loop-induced dipole antenna, we start from the vector potential for a magnetic current source as follows [1], referring to Fig. 3:

$$\mathbf{F}(x,y,z) = \frac{\varepsilon}{4\pi}\int_C \mathbf{I_m}(x',y',z')\frac{e^{-jkR}}{R}dl' \tag{1}$$

where k is the free-space propagation constant.

It can be shown that the vector potential $\mathbf{F}$ only has angular component, and in the far-field region, (1) can be simplified to

$$\begin{aligned}\mathbf{F}_{\boldsymbol{\phi}} &= \frac{d\varepsilon I_{m0}e^{-jkr}}{4\pi}\int_0^{2\pi}\cos\phi' e^{jkd\sin\theta\cos\phi'}d\phi' \\ &\cong j\frac{d\varepsilon I_{m0}e^{-jkr}}{2r}J_1(kd\sin\theta) \end{aligned}\tag{2}$$

where J_1 is the Bessel function of the first kind of order one. Using the far-field relation such that $\mathbf{H}_F \approx -j\omega\mathbf{F}$ and $\mathbf{E}_F \approx j\omega\eta\hat{\boldsymbol{a}}_{\boldsymbol{r}} \times \mathbf{F}$, where η is the free-space wave impedance, we can then obtain the electric and magnetic fields in the far field

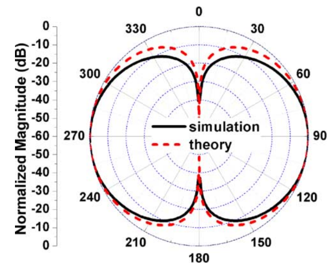

Fig. 4. Comparison between theory and EM simulation of the pattern.

$$H_r = H_\theta = 0 \tag{3a}$$

$$H_\phi = \frac{\omega d\epsilon I_{m0}e^{-jkr}}{2r}J_1(kd\sin\theta) \tag{3b}$$

$$E_r = E_\phi = 0 \tag{3c}$$

$$E_\theta = -\frac{\omega d\sqrt{\mu\varepsilon}I_{m0}e^{-jkr}}{2r}J_1(kd\sin\theta). \tag{3d}$$

Equation (3) can also be verified through the duality theorem of a uniform current-loop antenna [1]. The radiation intensity U of the antenna can then be obtained from (3d) as

$$U = \frac{r^2}{2\eta}|E_\theta|^2 = \frac{(\omega d)^2\sqrt{\mu}\varepsilon^{1.5}|I_{m0}|^2}{8}J_1^2(kd\sin\theta). \tag{4}$$

In order to verify the theoretical analysis for the proposed antenna, a full-wave simulation using the commercial electromagnetic (EM) simulator CST has been carried out. In the EM simulation, the dielectric constant of the substrate is 2.2, and the dimensions of the antenna as given in Fig. 1 are $W_1 = W_2 = 13$ mm, $L = 18$ mm, $h = 1.575$ mm, $a = 2.4$ mm, $b = 3.5$ mm. The simulated result of the normalized copolarization pattern at the yz-plane cut depicted in Fig. 1(a) is compared to the theoretical radiation pattern using (4). In this case, d is chosen to be equal to the average of a and b, which is 2.95 mm or $0.16225\lambda_0$, where λ_0 is the free-space wavelength of the center frequency 16.5 GHz of the antenna. The results are plotted in Fig. 4, and as one can observe, the agreement between the theory and EM simulation is very good, thereby confirming the proposed analysis for the antenna serves as a great approximation to find the radiated fields.

III. Simulations and Experimental Verifications

In order to further validate the proposed idea, prototypes of the antennas are fabricated and the experimental data are compared to the simulated results.

A. Single Element

The single element of the proposed magnetic-current-loop antenna has the same dimensions described in Section II. The substrate we use here is RT/Duroid 5880 with a thickness of 1.575 mm and a dielectric constant of 2.2. Fig. 5 illustrates the simulated 3-D radiation pattern of the antenna, clearly demonstrating a well-known donut-like shape that an electric dipole exhibits. The simulated gain of the antenna reads 2.75 dBi, and the simulated radiation efficiency including the matching effect is around 86%. The fabricated prototype of a single-element antenna is shown in Fig. 6(a) and (b); it is noted that solder is attached on top and bottom sides to ensure a good contact of vias of the SIW cavity.

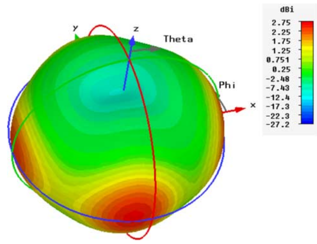

Fig. 5. Simulated 3-D radiation pattern of a single antenna.

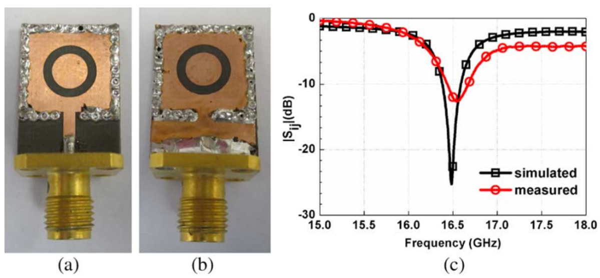

Fig. 6. Prototype of the single antenna: (a) front, (b) back side, and (c) its return loss.

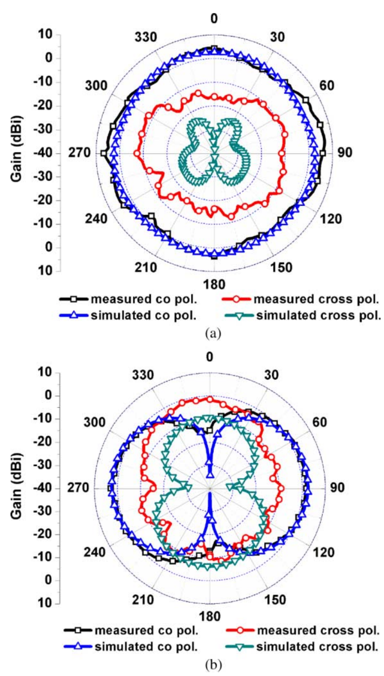

Fig. 7. Radiation patterns at (a) xy-plane and (b) yz-plane.

The return loss of the proposed antenna is measured and compared to the full-wave EM simulation as shown in Fig. 6(c). The dip of the S_{11} shifted slightly from 16.5 to 16.65 GHz in the measurement, showing the return loss is around 13 dB at the center frequency. It is worth mentioning that the center frequency of the proposed antenna is in fact higher than that of an SIW cavity with the same dimensions but without the annular ring slots. This is because the capacitance of the cavity resonator decreases when some the metal is removed from the top and bottom in the antenna's case.

The radiation patterns of the antenna have also been measured and compared to the simulation as shown in Fig. 7. In the horizontal cut (xy-plane), the antenna exhibits nearly an omnidirectional pattern as expected; the magnitude of cross polarization is around 20 dB less than the copolarization. In the vertical plane

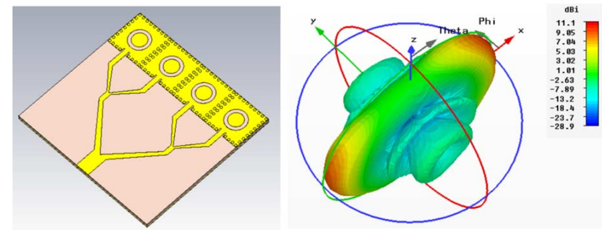

Fig. 8. Simulated 3-D radiation pattern of a single antenna.

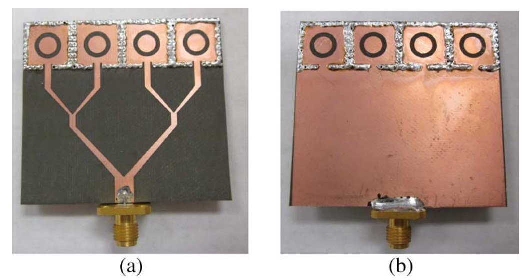

Fig. 9. Prototype of the four-element antenna array: (a) front and (b) back side.

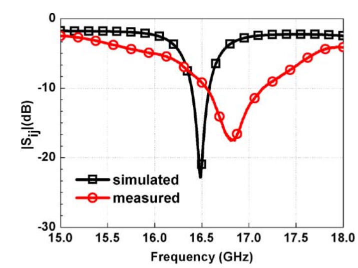

Fig. 10. Return loss

(yz-plane), the copolarization exhibits a donut-like pattern and has a null in the broadside. The cross-polarization level, however, appears higher in the measurement; this might be because the magnitude of the tangential E-field on the annular slot is not uniform and therefore cannot cancel well in the far field.

B. Array

Utilizing the proposed single element, we can realize an antenna array with a higher directivity. Fig. 8 shows the simulated 3-D radiation pattern of a four-element array with the elements side by side and excited with the same amplitude and phase. The simulated gain is around 11.1 dBi, and the simulated radiation efficiency is around 84%.

The prototype of a four-element array has also been fabricated using the same substrate and is shown in Fig. 9. A one-to-four power divider is used to equally excite each of the elements. Fig. 10 compares the simulated and measured return loss of the antenna array, indicating a frequency shift in the measurement of the center frequency from 16.5 to 16.8 GHz, which may be due to the handmade fabrication inaccuracy. The horizontal cut of the radiation pattern of the four-element array is shown in Fig. 11, indicating the array has a main beam of 10 dB gain. In addition, the cross-polarization level is around 20 dB less than the copolarization.

C. Mutual Coupling

The mutual coupling effect between the antenna elements has also been studied. Fig. 12 shows the fabricated two-element

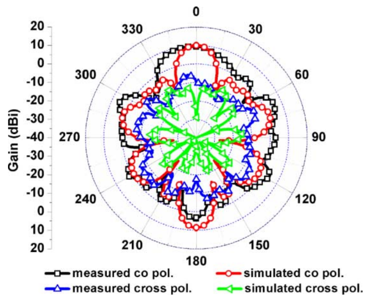

Fig. 11. Radiation patterns at xy-plane.

(a) (b)

Fig. 12. Prototype of the two-element antennas side by side: (a) front and (b) back side.

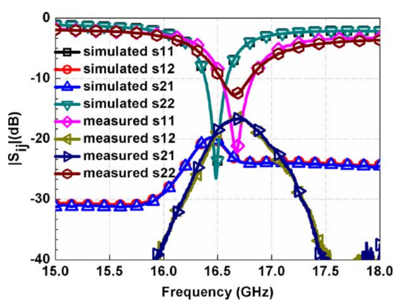

Fig. 13. S-parameters of the two-element side-by-side antennas.

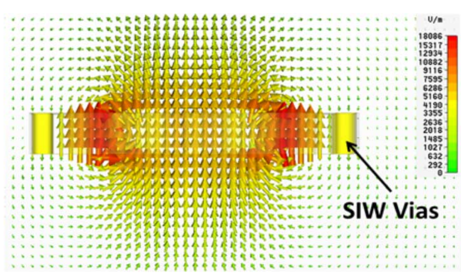

Fig. 14. Electric field distribution of the cross section of the antenna.

antennas side by side. The S-parameters of the two-element antenna are plotted in Fig. 13. There is some frequency shift between the simulation and measurement, which might be due to handmade fabrication errors; the measured S_{21} of the two elements is around -17 dB, showing a reasonably good isolation between the two elements.

IV. Top Metal and Ground Effect

Another advantage of the proposed antenna is that it is less sensitive to the surrounding metal as well as the size of the ground plane. The reason is because the E-field is oriented vertically and normal to the metal surfaces; therefore, it will not change the antenna's boundary condition as depicted in Fig. 14.

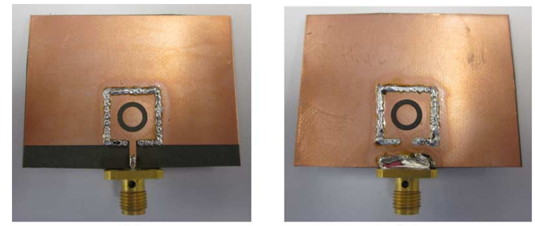

(a) (b)

Fig. 15. Prototype of the antenna with extra metal: (a) front and (b) back side.

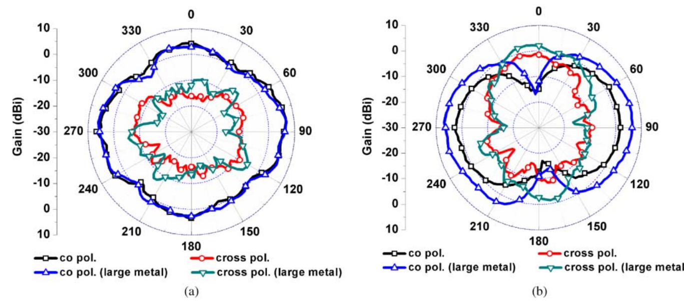

Fig. 16. Measured radiation patterns at (a) xy-plane and (b) yz-plane.

To compare, we fabricate another antenna with a larger metal on both of the top and bottom layers as shown in Fig. 15. The radiation patterns are plotted in Fig. 16 in comparison to the one with smaller ground plane as shown in Fig. 6. It can be observed that changing the metal size on the top and bottom layers does not have much effect on the radiation patterns.

V. Conclusion

A novel magnetic current loop-induced electric dipole is presented. The proposed antenna has a vertical polarization of E-field that is usually not available for low-profile printed antennas. A four-element array based on the proposed antenna is demonstrated to realize a high gain. In addition, we show that due to the E-field distribution, the proposed antenna is less sensitive to the surrounding metal and the ground plane. The proposed magnetic-current-loop dipole antenna is promising to be further used to build other types of antennas that use dipoles as fundamental elements. In addition, its potential applications can be external drop-in antennas for mobile devices.

References

[1] C. A. Balanis, *Antenna Theory*, 3rd ed. Hoboken, NJ, USA: Wiley.
[2] R. Waterhouse, *Printed Antennas for Wireless Communications*. Hoboken, NJ, USA: Wiley.
[3] J. Huang, "Circularly polarized conical patterns from circular microstrip antennas," *IEEE Trans. Antennas Propag.*, vol. AP-32, no. 9, pp. 991–994, Sep. 1984.
[4] L. Economou and R. J. Langley, "Patch antenna equivalent to simple monopole," *Electron. Lett.*, vol. 33, no. 9, pp. 727–729, Nov. 1999.
[5] C. B. Ravipati, "Compact circular microstrip antenna for conical pattern," in *IEEE AP-S Int. Symp. Dig.*, Jun. 2004, vol. 4, pp. 3820–3823.
[6] A. Al-Zoubi, F. Yang, and A. Kishk, "A broadband center-fed circular patch-ring antenna with a monopole like radiation pattern," *IEEE Trans. Antennas Propag.*, vol. 57, no. 12, pp. 789–792, Dec. 2009.
[7] D. Kim, J. W. Lee, C. S. Cho, and T. K. Lee, "X-band circular ring slot antenna embedded in single-layered SIW for circular polarization," *Electron. Lett.*, vol. 45, no. 13, pp. 668–669, Jun. 2009.
[8] J. Lacik, "Circularly polarized SIW square ring-slot antenna for X-band applications," *Microw. Opt. Technol. Lett.*, vol. 54, no. 11, pp. 2590–2594, 2012.